

Three-Dimensional Solution Structure of the E3-Binding Domain of the Dihydrolipoamide Succinyltransferase Core from the 2-Oxoglutarate Dehydrogenase Multienzyme Complex of *Escherichia coli*^{†,‡}

Mark A. Robien,[§] G. Marius Clore,^{*,§} James G. Omichinski,[§] Richard N. Perham,^{||} Ettore Appella,[⊥] Kazuyasu Sakaguchi,[⊥] and Angela M. Gronenborn^{*,§}

Laboratory of Chemical Physics, Building 2, National Institute of Diabetes and Digestive and Kidney Diseases, National Institutes of Health, Bethesda, Maryland 20892, and Laboratory of Cell Biology, Building 37, National Cancer Institute, National Institutes of Health, Bethesda, Maryland 20892

Received November 19, 1991; Revised Manuscript Received January 9, 1992

ABSTRACT: The three-dimensional solution structure of a 51-residue synthetic peptide comprising the dihydrolipoamide dehydrogenase (E3)-binding domain of the dihydrolipoamide succinyltransferase (E2) core of the 2-oxoglutarate dehydrogenase multienzyme complex of *Escherichia coli* has been determined by nuclear magnetic resonance spectroscopy and hybrid distance geometry-dynamical simulated annealing calculations. The structure is based on 630 approximate interproton distance and 101 torsion angle (ϕ , ψ , χ_1) restraints. A total of 56 simulated annealing structures were calculated, and the atomic rms distribution about the mean coordinate positions for residues 12-48 of the synthetic peptide is 1.24 Å for the backbone atoms, 1.68 Å for all atoms, and 1.33 Å for all atoms excluding the six side chains which are disordered at χ_1 and the seven which are disordered at χ_2 ; when the irregular partially disordered loop from residues 31 to 39 is excluded, the rms distribution drops to 0.77 Å for the backbone atoms, 1.55 Å for all atoms, and 0.89 Å for ordered side chains. Although proton resonance assignments for the N-terminal 11 residues and the C-terminal 3 residues were obtained, these two segments of the polypeptide are disordered in solution as evidenced by the absence of nonsequential nuclear Overhauser effects. The solution structure of the E3-binding domain consists of two parallel helices (residues 14-23 and 40-48), a short extended strand (24-26), a five-residue helical-like turn, and an irregular (and more disordered) loop (residues 31-39). This report presents the first structure of an E3-binding domain from a 2-oxo acid dehydrogenase complex. Related domains from the E2 chains of other 2-oxo acid dehydrogenase complexes are likely to be structurally analogous, given their marked sequence similarity and the presence of a number of conserved residues at pivotal positions. This is particularly true for the *E. coli* pyruvate dehydrogenase complex since the E3 component which is bound by its dihydrolipoamide acetyltransferase core is identical to that bound by the dihydrolipoamide succinyltransferase core of the 2-oxoglutarate dehydrogenase complex.

The 2-oxoglutarate dehydrogenase (2-OGDH), pyruvate dehydrogenase (PDH), and branched-chain 2-oxo acid dehydrogenase multienzyme complexes are responsible for the oxidative decarboxylation of different 2-oxo acid substrates, resulting in acyl-CoA products [see Reed and Hackert (1990), Patel and Roche (1990), and Perham (1991) for recent reviews]. 2-OGDH and PDH complexes are prominent members of the primary energy-producing pathways of glycolysis and the tricarboxylic acid cycle, and the branched chain 2-oxo acid dehydrogenase fulfills a similarly important role in the pathways for the catabolism of valine, isoleucine, and leucine. The structural and functional properties of these enzyme

complexes from eukaryotic and prokaryotic species have been widely studied, disclosing some striking similarities in their overall design. In each case, the core of the complexes is composed of either 24 or 60 copies of the enzyme responsible for the acyltransferase (E2) reaction arranged with octahedral or icosahedral symmetry, respectively; another E2-like component, known as component X, appears to be a critical additional structural element in at least the icosahedral PDH complexes from eukaryotic species, even though it probably lacks the E2-catalytic activity. Covalently bound substrate intermediates are shuttled from the E1 subunit (a decarboxylase) to the E2 subunit (an acyltransferase) while attached to a ~ 14 Å long lipoylated lysine residue (a "swinging arm") on E2, and then the reduced dihydrolipoamide is reoxidized by the E3 (dihydrolipoamide dehydrogenase) component.

The 2-oxoglutarate dehydrogenase complex of (2-OGDH) *Escherichia coli* ($M_r \sim 5 \times 10^6$) is composed of three subunit enzymes: E1₀, 2-oxoglutarate decarboxylase [2-oxoglutarate dehydrogenase (lipoamide), EC 1.2.4.2]; E2₀, dihydrolipoamide succinyltransferase (EC 2.3.1.61); and E3, dihydrolipoamide dehydrogenase (EC 1.8.1.4). (In discussing the subunits of the different 2-oxo acid dehydrogenase complexes, this paper will follow the convention that the suffixes -o, -p, and -b will be added when referring to an enzyme from the 2-OGDH, PDH, and branched chain 2-oxo acid de-

[†]This work was supported by the AIDS Targeted Antiviral Program of The Office of the Director of the National Institutes of Health (G. M.C. and A.M.G.). M.A.R. was supported by the Howard Hughes Medical Institute-National Institutes of Health Research Scholars Program, and R.N.P. was supported by the Fogarty Scholars-in-Residence Program of the National Institutes of Health.

[‡]The coordinates of the 56 final simulated annealing structures of the E3-binding domain of the dihydrolipoamide succinyltransferase core from the 2-oxoglutarate dehydrogenase multienzyme complex of *E. coli*, as well as those of the restrained minimized mean structure, have been deposited in the Brookhaven Protein Data Bank, along with the complete list of experimental restraints used in the calculations.

[§]NIDDK, NIH.

^{||}Permanent address: Department of Biochemistry, University of Cambridge, Tennis Court Road, Cambridge CB2 1QW, U.K.

[⊥]NCI, NIH.

hydrogenase complexes, respectively.) The *E. coli* 2-OGDH complex contains 24 copies of the E2o subunit as an octahedral core that forms a truncated cube of dimension $149 \pm 15 \text{ \AA}$ (Reed, 1974); homodimers of E1o and E3 subunits aggregate peripherally around this E2o core. Approximately full activity of the enzyme complex has been demonstrated with 6 E1o dimers and 6 E3 dimers bound, although other experiments have shown that the isolated E2o core can bind up to 18 E1o dimers (Reed, 1974). Electron microscopy and low-resolution (ca. 18 Å) X-ray diffraction studies of proteolyzed complexes have suggested that E3 binds diagonally to the faces of the truncated cube, thus reducing the symmetry of the E3-E2 complex to that of space group $P2_13$; furthermore, it is believed that E1 probably binds to the edges of the cube (Oliver & Reed, 1982; Yang et al., 1985; Wagenknecht et al., 1987; Reed & Hackert, 1990).

The E2 chain has attracted particular attention because of the multiple critical design features that it embodies. Three domains of the E2o chain have been identified by limited proteolysis experiments on the *E. coli* 2-OGDH complex. The *E. coli* E2o chain contains an N-terminal domain (approximately 80 residues) with a single lipoylated lysine residue and a larger C-terminal domain (approximately 300 residues) with E1o- and E2o-binding sites and succinyltransferase activity. Between these two domains is a small folded domain of approximately 50 amino acids which is believed to contain a site necessary for binding E3 to the E2o core since limited proteolysis conditions that detach this middle domain from the core also cause release of E3; moreover, this fragment selectively binds E3 (Packman & Perham, 1986). It has also been suggested that this fragment may play a role in binding E1, although perhaps only in icosahedral complexes (Behal et al., 1989; Perham, 1991). On both sides of the central E3-binding domain are interdomain segments of polypeptide chain which are particularly rich in certain amino acids such as alanine, proline, and those with charged side chains. Conformational flexibility in these segments is believed to account for the extremely sharp high-field (methyl) resonances noted in the 1D ^1H NMR spectra of intact 2-oxo acid dehydrogenase complexes (Perham et al., 1981; Texter et al., 1988; Radford et al., 1989a) and to facilitate the movement of the lipoyl domains between the successive active sites as a crucial part of the enzymic mechanism (Radford et al., 1989b; Perham, 1991). The interdomain segments appears to be conformationally extended as well as flexible (Radford et al., 1989a; Wagenknecht et al., 1990), which may help to keep the domains apart while still allowing them to move as required. The E2 chains of the PDH and branched-chain 2-oxo acid dehydrogenase complexes have analogous structures, except that among the PDH complexes the number of lipoyl domains per chain can vary from one to three according to the phylogeny of the source (Perham & Packman, 1989; Reed & Hackert, 1990; Perham, 1991).

Current knowledge about the structure of the E2 core or the interface between E2 and E3 is limited, in large part because of the lack of crystals of the intact enzyme complexes (DeRosier et al., 1971; DeRosier & Oliver, 1971), which may be attributable to the flexible regions linking the lipoyl domains at or near the surface of the enzyme particles. However, X-ray structures of the dimeric E3 subunits from *Saccharides cerevisiae* (4.5-Å resolution; Takanaka et al., 1988) and *Azotobacter vinelandii* (2.2-Å resolution; Mattevi et al., 1991) have been published. The domain-and-linker structure of the E2 chain has motivated us to employ an alternative approach, namely, NMR spectroscopy, to study individual domains de-

rived from E2. Progress has already been made with the lipoyl domain (Dardel et al., 1990, 1992). In this paper, we present the determination of the solution structure of a synthetic peptide comprising the E3-binding domain of the lipoyl succinyltransferase core, E2o, from *E. coli* 2-OGDH, thereby providing high-resolution conformational details of a key structural element of this multienzyme complex.

EXPERIMENTAL PROCEDURES

Peptide Synthesis. The peptide studied comprises the amino acid sequence from position 103 to 152 deduced from the DNA sequence of the gene encoding the E2o chain of the *E. coli* 2-OGDH complex reported by Spencer et al. (1984), with an additional Tyr added at the N-terminus. It incorporates the E3-binding domain as defined by limited proteolysis of the intact complex (Packman & Perham, 1986, 1987). It was prepared by solid-phase peptide synthesis (Merrifield et al., 1982) on an Applied Biosystems 430A peptide synthesizer. The final protected resin was cleaved by using the low/high HF cleavage method (Tam et al., 1983). The extracted peptide (5% aqueous acetic acid) was purified by HPLC on a Vydac C4 semipreparative reverse-phase column using an acetonitrile-water solvent gradient containing 0.1% trifluoroacetic acid. The identity of the synthetic peptide was established by amino acid sequence analysis, mass spectrometry, and by the NMR assignment procedure. Samples for NMR spectroscopy contained 2 mM peptide in either 99.996% D_2O or 90% $\text{H}_2\text{O}/10\% \text{D}_2\text{O}$ at pH 5.3.

NMR Spectroscopy. The following spectra were recorded at 600 MHz on a Bruker AM600 spectrometer at 15 and/or 25 °C in both H_2O and D_2O : HOHAHA (Braunschweiler & Ernst, 1983; Davis & Bax, 1985) with mixing times ranging from 18 to 51 ms, NOESY (Jeener et al., 1979) with mixing times of either 50 or 150 ms, P.COSY (Marion & Bax, 1988), and PE-COSY (Mueller, 1987) with a 35° mixing pulse. All spectra were recorded in pure phase absorption mode using the time-proportional incrementation method (Marion & Wüthrich, 1983). HOHAHA spectra were recorded with a WALTZ17y anisotropic mixing sequence sandwiched between 1.5-ms trim pulses (Bax, 1989). Water suppression for the NOESY and HOHAHA spectra was achieved using a semi-selective jump-return read sequence (Platéau & Guéron, 1982; Bax et al., 1987), while the COSY-type spectra employed weak presaturation together with the SCUBA technique (Brown et al., 1987). $^3J_{\text{HN}\alpha}$ coupling constants were derived from the P.COSY spectra recorded in water as described previously (Forman-Kay et al., 1990; Omichinski et al., 1990).

NMR Assignments. Sequential resonance assignment was accomplished by conventional 2D NMR methods (Wüthrich, 1986; Clore & Gronenborn, 1987, 1989). Through-bond connectivities were established from HOHAHA and COSY-type spectra, while through space connectivities were identified from the NOESY spectra. Examples of the 150-ms mixing time NOESY spectrum recorded in H_2O are shown in Figure 1; a schematic summary of the short-range NOEs is shown in Figure 2. Stereospecific assignments and ϕ , ψ , and χ_1 torsion angle restraints were obtained from $^3J_{\alpha\beta}$ and $^3J_{\text{NH}\alpha}$ constants derived from the PE-COSY and P.COSY spectra, respectively, and intraresidue and sequential NOEs observed in the 50-ms mixing time NOESY involving the NH, C^αH , and C^βH protons, employing the conformational search program STEREOSEARCH (Nilges et al., 1990). A complete list of assignments is presented in Table I.

The most distinctive features of the secondary structure, namely, the two short helices from residues 13–23 and 40–48, are evident from a qualitative interpretation of the short-range

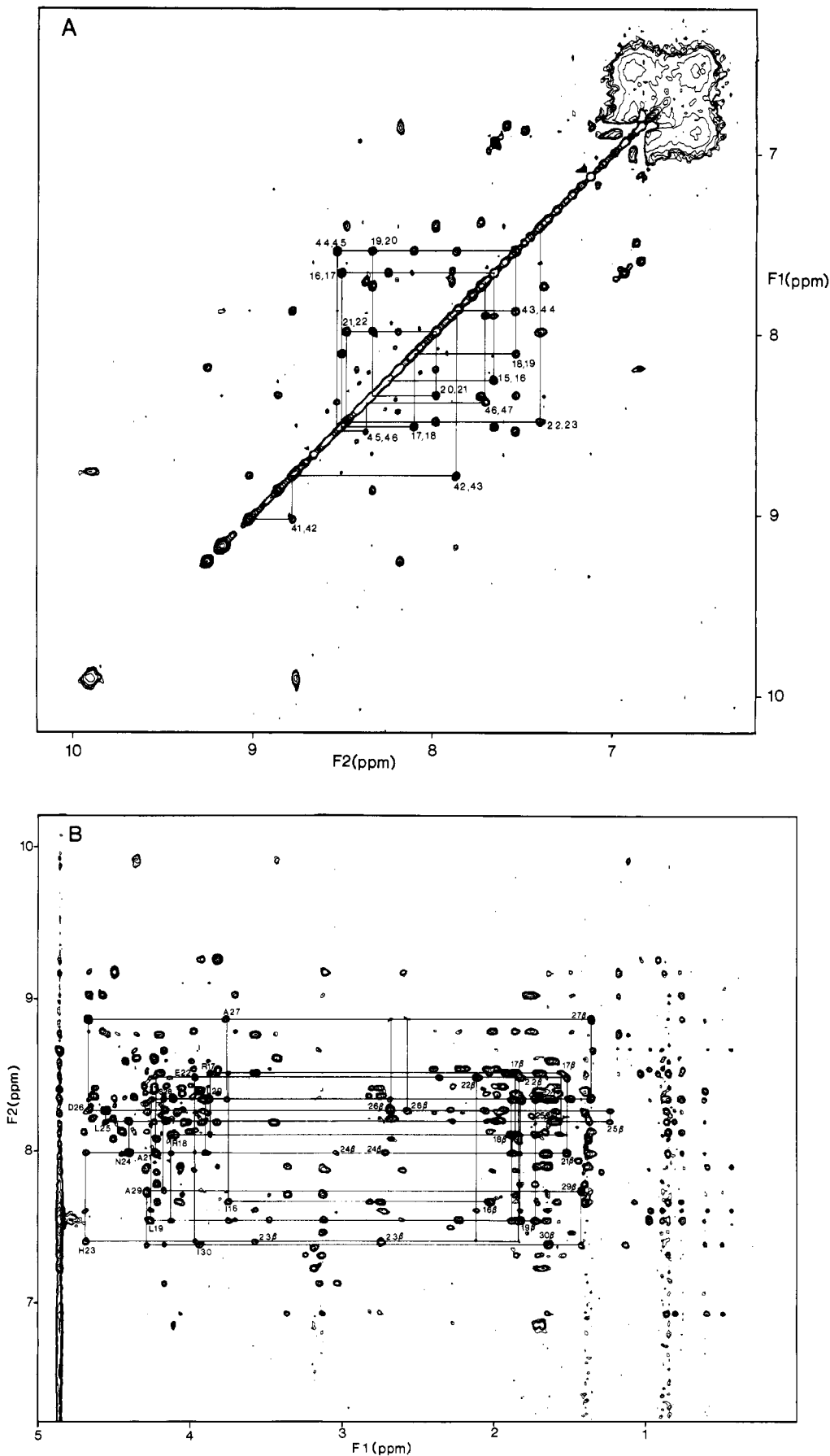


FIGURE 1: (A) NH(F_2 axis)-NH(F_1 axis) and (B) NH(F_2 axis)-aliphatic (F_1 axis) regions of the 600-MHz NOESY spectrum (150-ms mixing time) of the E3-binding domain (2 mM) recorded in 90% H_2O /10% D_2O at 25 °C and pH 5.3. A series of NH(i)-NH($i+1$) and $C^\alpha H(i)$ -NH($i+1$) sequential NOE connectivities are indicated in panels A and B, respectively. Also shown in panel B are some $C^\beta H(i)$ -NH($i+1$) NOEs. Residue labels in panel B are at the position of the intraresidue $C^\alpha H(i)$ -NH(i) and $C^\beta H(i)$ -NH(i) cross peaks, the latter denoted by the letter β .

Table I: Protein Resonance Assignments of the E3-Binding Domain of E2o at 25 °C, pH 5.3^a

residue	NH	C ^α H	C ^β H	other
Tyr-1		4.20	3.16, 3.07	C ^β H 7.11, 7.11; C ^γ H 6.82, 6.82
Ala-2	8.56	4.39	1.36	
Ser-3	8.28	4.45	3.99, 3.89	
Leu-4	8.47	4.27	1.64, 1.60	C ^γ H 1.63; C ^δ H 0.92, 0.87
Glu-5	8.37	4.19	2.03, 1.96	C ^γ H 2.29, 2.29
Glu-6	8.15	4.20	2.08, 2.00	C ^γ H 2.29, 2.29
Gln-7	8.21	4.14	2.09, 1.96	C ^γ H 2.32; N ^H 7.44*, 6.82
Asn-8	8.37	4.67	2.84, 2.79	N ^δ H 7.59*, 6.90
Asn-9	8.34	4.68	2.84, 2.78	N ^δ H 7.59*, 6.90
Asp-10	8.19	4.53	2.73, 2.68	
Ala-11	8.04	4.24	1.39	
Leu-12	7.92	4.45	1.69*, 1.39	C ^γ H 1.65; C ^δ H 0.87, 0.87 ^b
Ser-13	8.06	4.71	4.28, 4.01	
Pro-14		4.29	2.42, 2.07*	C ^γ H 2.21, 2.21; C ^δ H 3.99, 3.91
Ala-15	8.17	4.11	1.41	
Ile-16	7.60	3.79	2.04	C ^γ H 1.61, 1.15; C ^γ mH 0.90; C ^δ H 0.80
Arg-17	8.43	3.89	1.87*, 1.59	C ^γ H 1.73, 1.73; C ^δ H 3.27, 3.18; N ^H 7.27
Arg-18	8.04	4.14	1.91*, 1.75	C ^γ H 1.60, 1.60; C ^δ H 3.21, 3.21; N ^H 7.27
Leu-19	7.52	4.25	1.85, 1.71*	C ^γ H 1.70; C ^δ H 0.99*, 0.92
Leu-20	8.30	3.96	1.92, 1.75	C ^γ H 1.84; C ^δ H 0.90*, 0.85
Ala-21	7.95	4.25	1.53	
Glu-22	8.39	4.01	2.13, 1.90*	C ^γ H 2.40, 2.40
His-23	7.46	4.70	3.57, 2.81*	C ^{δ2} H 7.61; C ^{δ1} H 8.69
Asn-24	7.99	4.44	3.05, 2.74	C ^δ H 7.42*, 6.82
Leu-25	8.16	4.53	1.61*, 1.31	C ^γ H 1.63; C ^δ H 0.90, 0.85*
Asp-26	8.22	4.69	2.71, 2.61	
Ala-27	8.76	3.83	1.38	
Ser-28	8.33	4.22	3.95, 3.90	
Ala-29	7.71	4.33	1.43	
Ile-30	7.37	3.96	1.68	C ^γ H 1.23, 0.57; C ^γ mH 0.66; C ^δ H 0.45
Lys-31	8.33	4.28	1.78, 1.78	C ^γ H 1.45, 1.45; C ^δ H 1.72, 1.72; C ^ε H 2.98
Gly-32	8.50	4.34, 3.63*		
Thr-33	9.67	4.52	4.46	C ^γ H 1.16
Gly-34	8.68	4.20, 3.63		
Val-35	8.39	3.86	1.96	C ^γ H 1.05, 0.95*
Gly-36	9.10	3.94, 3.86		
Gly-37	8.17	4.02*, 3.53		
Arg-38	6.94	4.15	1.75, 1.75	C ^γ H 1.70, 1.70; C ^δ H 3.21, 3.21; N ^H 7.19
Leu-39	8.30	4.52	1.65, 1.52	C ^γ H 1.68; C ^δ H 0.92*, 0.87
Thr-40	9.05	4.65	4.57	C ^γ H 1.21
Arg-41	8.94	3.77	1.80, 1.80	C ^γ H 1.53, 1.53; C ^δ H 3.17, 3.17; N ^H 7.43
Glu-42	8.75	4.02	2.04*, 1.90	C ^γ H 2.27, 2.27
Asp-43	7.87	4.35	3.10*, 2.65	
Val-44	7.57	3.55	2.25	C ^γ H 1.01, 0.81*
Glu-45	8.50	3.87	2.06, 2.06	C ^γ H 2.41, 2.23
Lys-46	8.29	4.08	1.87, 1.87	
His-47	7.77	4.35	3.36*, 3.14	C ^{δ2} H 7.00; C ^{δ1} H 8.40
Leu-48	7.86	4.12	1.72*, 1.42	C ^γ H 1.67; C ^δ H 0.63, 0.53*
Ala-49	7.68	4.24	1.40	
Lys-50	7.80	4.25	1.85, 1.75	C ^γ H 1.45, 1.45
Ala-51	7.81	4.10	1.32	

^a Chemical shifts are reported with respect to 4,4-dimethyl-4-silapentane-1-sulfonate. Stereospecific assignments are denoted as follows: for the C^β methylene protons, the asterisk indicates the H^{β3} proton; for the C^α methylene protons of Gly, the asterisk indicates the H^{α1} proton; for the NH₂ protons of Asn and Gln, the asterisk indicates the H^{β21} proton that is cis to C^β and the H^{α21} proton that is cis to C^γ, respectively; for the methyl protons of Val and Leu, the asterisk refers to the C^{γ1} and C^{δ1} methyl group, respectively. ^b At 15 °C, pH 5.3, the two methyl resonances of Leu-12 are no longer degenerate and have shifts of 0.86 and 0.76 for the C^{δ2} and C^{δ1} methyl groups, respectively.

of NOEs, in particular the consecutive stretch of relatively strong NH(*i*)-NH(*i*+1) NOEs together with the presence of C^αH(*i*)-C^βH(*i*+3) NOEs and C^αH(*i*)-NH(*i*+2,3,4) NOEs.

Structure Calculations and Experimental Restraints.

Structures were computed from the experimental NMR data using the hybrid distance geometry-dynamical simulated annealing method of Nilges et al. (1988a). This makes use of the program DISGEO (Havel & Wüthrich, 1984; Havel, 1986) to calculate an initial set of substructures comprising about one-third of the atoms by projection from *n*-dimensional distance space into Cartesian coordinate space, followed by simulated annealing with all atoms using the program XPLOR (Brünger et al., 1986; Brünger, 1988). The dynamical simulated annealing protocol involves minimization of a target function comprising quadratic harmonic terms for bonds, angles, improper torsion angles (which relate to planarity and

chirality restraints), a quartic van der Waals repulsion term for the nonbonded contacts, and square-well quadratic potential terms for interproton distance and torsion angle restraints (Nilges et al., 1988a-c). No electrostatic, hydrogen-bonding, or 6-12 Lennard-Jones van der Waals energy terms are used in the simulated annealing calculations.

NOEs were identified in the 150-ms NOESY spectra and classified on the basis of the 50- and 150-ms NOESY spectra into strong, medium, weak, and very weak, corresponding to interproton distance restraints of 1.8-2.8, 1.8-3.3, 1.8-5.0, and 2.5-6.0 Å, respectively (Williamson et al., 1985; Clore et al., 1986). Upper limits for nonstereospecifically assigned methylene protons and methyl protons were corrected appropriately for center averaging (Wüthrich et al., 1983). In addition, 0.5 Å was added to the upper limits of distances involving methyl protons (Clore et al., 1987; Wagner et al.,

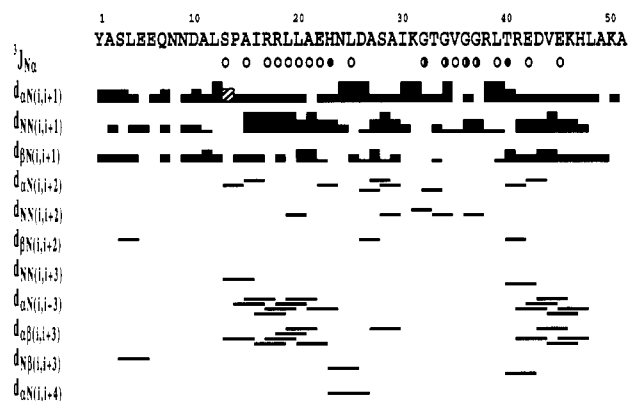


FIGURE 2: Summary of the short-range NOEs involving the NH, C α H, and C β H protons, as well as the C δ H protons of proline, and of the $^3J_{\text{HN}\alpha}$ coupling constants. The C α H(*i*)-C δ H(*i*+1) NOE is shown as a hatched box along the same line as the C α H(*i*)-NH(*i*+1) connectivities. The thickness of the lines reflects the intensity of the NOEs. $^3J_{\text{HN}\alpha}$ less than 6 Hz and greater than 8 Hz are represented as open and closed circles, respectively. In the case of the Gly residues, with one $^3J_{\text{HN}\alpha}$ > 8 Hz and the other < 6 Hz, a half-open circle is used.

1987). The minimum ranges employed for the ϕ , ψ , and χ_1 torsion angle restraints derived from the program STEREOSEARCH (Nilges et al., 1990) were $\pm 30^\circ$, $\pm 50^\circ$, and $\pm 20^\circ$, respectively (Kraulis et al., 1989), except for Pro, where a range of $\pm 20^\circ$ for ϕ was used. All peptide bonds were restrained to be trans.

As described in previous structure determinations from this laboratory (Kraulis et al., 1989; Omichinski et al., 1990; Forman-Kay et al., 1991; Clore et al., 1990, 1991; Gronenborn et al., 1991), an iterative strategy was employed by carrying out a series of successive calculations with more restraints incorporated at each successive stage. Analysis of the initial low-resolution (determinacy) structures allowed the identification of additional interproton distance restraints and stereospecific assignments, as well as verification of the existing restraints. The final simulated annealing (SA) structures were calculated on the basis of 630 approximate interproton distance restraints, made up of 169 sequential ($|i - j| = 1$), 102 medium range ($1 < |i - j| \leq 5$), and 44 long-range ($|i - j| > 5$) interresidue NOEs and 315 intraresidue NOEs and 101 torsion angle restraints comprising 46 ϕ , 35 ψ , and 20 χ_1 angles. (The complete list of restraints has been deposited in the Brookhaven

Protein Data Bank together with the coordinates.) The interproton distances include NOEs to 12 stereospecifically assigned β -methylene protons (out of a total of 33 β -methylene groups), to the stereospecifically assigned α -methylene protons of two of the three Gly residues, to the stereospecifically assigned methyl groups of the two valine residues, and to the stereospecifically assigned methyl groups of six (all except Leu-4) of the seven Leu residues. It should be noted that all the β -methylene protons that could not be stereospecifically assigned involve residues with disordered χ_1 side chain torsion angles, as judged by $^3J_{\alpha\beta}$ coupling constant values of 6–8 Hz. No hydrogen-bonding restraints were used, as backbone amide exchange was too fast to observe any NH resonances more than 2 h after dissolving lyophilized peptide in D $_2$ O.

RESULTS AND DISCUSSION

The Converged Structures. A total of 56 SA structures were calculated, and superpositions of the backbone atoms are shown in Figure 3. The structural statistics are summarized in Table II, and the atomic rms distribution of the individual structures about the mean coordinate positions as a function of residue number is shown in Figure 4. All the structures satisfy the experimental restraints with no interproton distance or torsion angle violations greater than 0.3 Å and 1°, respectively, and the deviations from idealized covalent geometry are small. In addition, the nonbonded contacts are good as judged by the calculated Lennard-Jones van der Waals energy, which has an average value of -104.0 ± 9.7 kcal·mol $^{-1}$, and the ϕ, ψ angles of all the residues in the ordered regions of the structure lie in the allowed regions of the Ramachandran plot.

The precision of the atomic coordinates can be assessed from the atomic rms distribution about the mean coordinate positions (cf. Table II and Figure 4). This shows that the N- and C-termini are very poorly defined and that the orientation of the irregular loop from residues 31–38 relative to the main body of the protein cannot be determined from the present data. The same picture emerges from the values of the mean of the angular deviation (Zar, 1986) for the backbone ϕ and ψ angles. The ordered portion of the structure from 14 ϕ to 31 ϕ and from 38 ψ to 48 ϕ has a mean ϕ, ψ angular deviation of $15.7^\circ \pm 5.1^\circ$. Similar low values are obtained when the regions of regular secondary structure are analyzed individually. The irregular loop (31 ψ to 38 ϕ), on the other hand,

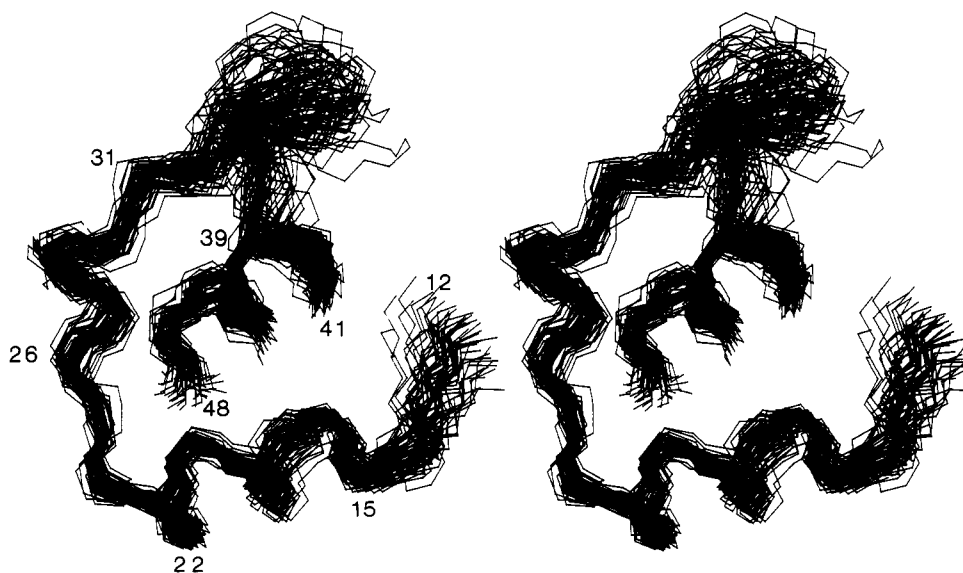


FIGURE 3: Stereoview showing a best fit superposition of the backbone atoms of the 56 final SA structures (residues 12–48) of the *E. coli* E3-binding domain of E2o.

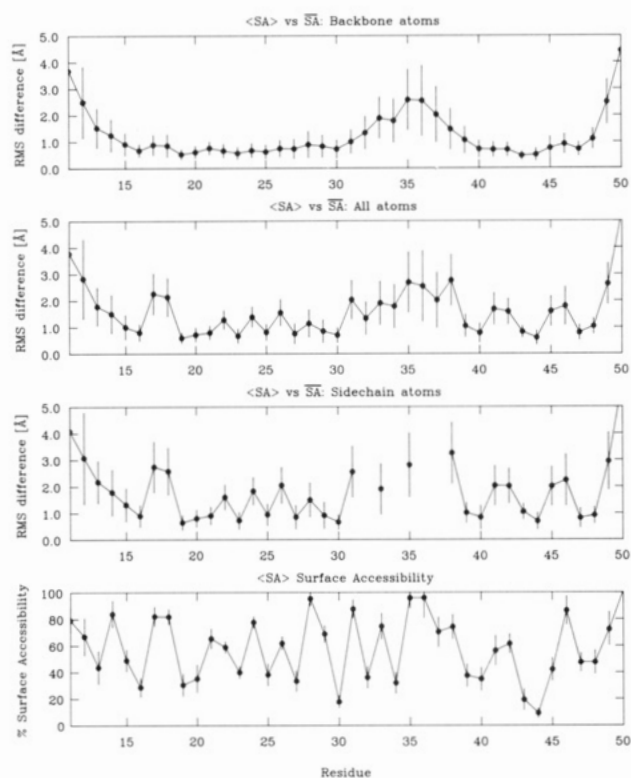


FIGURE 4: Atomic rms distribution of the 56 individual SA structures about the mean structure, \overline{SA} , for backbone atoms, all atoms, and side-chain atoms as a function of residue number, together with the mean surface accessibility of each residue. The mean values are represented as solid circles, and the error bars indicate the standard deviations in these values.

has a mean ϕ, ψ angular deviation of $35.4^\circ \pm 12.1^\circ$, while the highly disordered C- and N-termini of the synthetic peptide (1 ψ to 13 ψ and 48 ψ to 51 ϕ) exhibit a mean ϕ, ψ angular deviation of $48.1^\circ \pm 17.0^\circ$.

Description of the Structure. The overall folding topology of the E3-binding domain of the *E. coli* E2o chain is illustrated by the backbone atom superpositions of the individual SA structures in Figure 3 and by the schematic ribbon drawing of the restrained minimized mean (\overline{SA})r structure in Figure 5. The structure consists of two parallel helices (residues 14–23 and 40–48) at an angle of approximately 25° , two short extended strands (residues 12–13 and 24–26), a well-ordered five-residue helix-like turn (26–30), and an irregular and more disordered loop (residues 31–39). The five-residue turn starts out with 3_{10} helix character and finishes with type I β -turn character, as evidenced by the $(-60^\circ, -30^\circ)$ ϕ, ψ angles of Asp-26 and Ala-27, and the $(-90^\circ, -60^\circ)$ ϕ, ψ angles of Ser-28. The irregular loop appears to form a finger-like structure, consisting of two antiparallel extended regions (residues 31–33 and 38–40) with a tight turn at the tip of the finger (residues 34–37). The N-terminal 11–13 residues and the C-terminal three residues are disordered, as judged by the almost complete absence of any medium- or long-range NOEs, although it was possible to obtain ^1H resonance assignments for these residues. It should be noted that the relative disorder of the C- and N-termini and the irregular loop confirms the dictum that the precision and accuracy of NMR-derived structures is directly correlated to the number of restraints (Clare & Gronenborn, 1989, 1991a,b).

Most of the ordered side chains are in the hydrophobic interior of the structure which consists of Ile-16, Leu-19, Leu-20, His-23, Leu-25, Ala-27, Ile-30, Leu-39, Val-44, and perhaps the hydrophobic hydrocarbon chain areas of Arg-41;

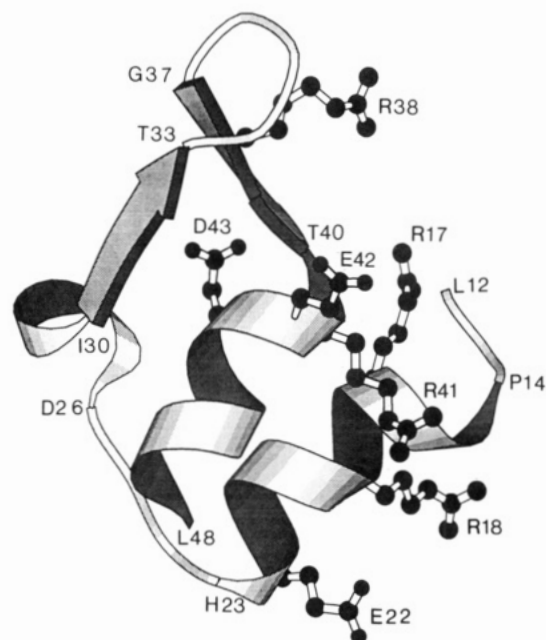


FIGURE 5: Schematic ribbon drawing of the restrained minimized mean (\overline{SA})r structure. Side chains of conserved charged residues are also shown. This schematic was produced with the program MOLSCRIPT (Kraulis, 1991).

of these residues, Leu-19, His-23, Ala-27, and Arg-41 are more peripherally situated around the hydrophobic core (Figure 6). The majority of the remaining side chains are disordered around χ_1 , as judged by $^3J_{\alpha\beta}$ coupling constant values of 6–8 Hz, consistent with their high surface exposure (Figure 4).

Comparison of the E3-Binding Domain of E2o with Those of Other E2 Sequences: Predictions of Structural Features. An alignment of the amino acid sequences of the E3-binding domains of the E2o, E2p, and E2b chains from several eukaryotic and prokaryotic species is shown in Figure 7. These sequences are aligned relative to the *E. coli* E2o sequence in such a manner as to give strict sequence identity at the N-termini of the two helices and similarity at positions close to the C-termini of the two helices.

Comparison of the aligned sequences reveals several residues that are either absolutely conserved or highly conserved. Four patterns emerge from a consideration of the aligned sequence and the structure.

The hydrophobic core, including the interhelical contacts, is quite highly conserved in all the sequences shown. Thus, in all the sequences presented, there are hydrophobic residues at the positions corresponding to Ile-16, Leu-20, Leu-25, Ala-27, Ile-30, Leu-39, and Val-44. Given their lack of surface accessibility (cf. Figure 4) and the observation that they constitute the hydrophobic interhelical contacts between helices I and II (Figure 6), it seems likely that they play a crucial role in determining and stabilizing the polypeptide fold.

There is sequence conservation at the positions corresponding to those residues which have positive ϕ angles in tight turns. Gly and Asn are the two amino acids that are most commonly found in these positions with positive ϕ angles (Richardson, 1981); 13 of the 15 sequences have a Gly or an Asn at residue 24 in the tight turn following helix I. The other tight turn which is located at the tip of the irregular loop has an absolutely conserved Gly at position 37 in all the sequences listed.

Proline, which can be regarded as a structurally restrictive amino acid, occurs at position 14 in the *E. coli* E3-binding domain and is also absolutely conserved in all the sequences

Table II: Structural Statistics and Atomic rms Differences^a

(A) Structural Statistics						
	(SA)		$\overline{\text{SA}}$		$\overline{\text{SA}}_r$	
rms deviations from experimental distance restraints (\AA) ^b						
all (630)	0.005 \pm 0.003		0.002		0.002	
interresidue sequential ($ i - j = 1$) (169)	0.005 \pm 0.004		0.002		0.001	
interresidue medium range ($1 < i - j \leq 5$) (102)	0.005 \pm 0.004		0.004		0.004	
interresidue long range ($ i - j > 5$) (44)	0.003 \pm 0.005		0.001		0.004	
intraresidue (315)	0.105 \pm 0.009		0.004		0.004	
rms deviations from experimental dihedral restraints (deg) (110) ^{b,c}						
F_{NOE} (kcal·mol ⁻¹) ^d	0.632 \pm 0.745		0.766		0.766	
F_{tor} (kcal·mol ⁻¹) ^d	0.014 \pm 0.014		0.000		0.000	
F_{repel} (kcal·mol ⁻¹) ^d	3.293 \pm 0.981		2.714		2.714	
E_{L-J} (kcal·mol ⁻¹) ^e	-92.0 \pm 8.7		-101.7		-101.7	
deviations from idealized covalent geometry						
bonds (\AA) (779)	0.003 \pm 0.000		0.003		0.003	
angle (deg) (1409)	1.675 \pm 0.003		1.675		1.675	
improper (deg) (278) ^f	0.468 \pm 0.006		0.476		0.476	

	(B) Atomic rms Differences (\AA)					
	residues 12-48			residues 14-30 and 39-47		
	backbone atoms	all atoms	all excluding disordered side chains ^g	backbone atoms	all atoms	all excluding disordered side chains ^g
$\langle \text{SA} \rangle$ vs $\overline{\text{SA}}$	1.24 \pm 0.36	1.68 \pm 0.32	1.33 \pm 0.34	0.77 \pm 0.23	1.55 \pm 0.26	0.89 \pm 0.22
$\langle \text{SA} \rangle$ vs $\overline{\text{SA}}_r$	1.31 \pm 0.36	1.81 \pm 0.33	1.42 \pm 0.34	0.80 \pm 0.23	1.73 \pm 0.26	0.94 \pm 0.22
$\overline{\text{SA}}_r$ vs $\overline{\text{SA}}$	0.42	0.69	0.50	0.22	0.77	0.30

^aThe notation of the structures is as follows: $\langle \text{SA} \rangle$ are the 56 final simulated annealing structures; $\overline{\text{SA}}$ is the mean structure obtained by averaging the coordinates of residues 14-30 and 39-47 of the individual 56 SA structures best fitted to each other; $\overline{\text{SA}}_r$ is the restrained minimized structure obtained by restrained minimization of $\overline{\text{SA}}$ (Nilges et al., 1988a). The number of terms for the various restraints is given in parentheses. ^bNone of the structures exhibited interproton distance violations greater than 0.3 \AA or dihedral angle violations greater than 1°. ^cThe torsion angle restraints comprise 46 ϕ , 35 ψ , and 20 χ_1 angles. ^dThe values of the square-well NOE and torsion angle potentials [cf. eqs 2 and 3 of Clore et al. (1986)] are calculated with force constants of 50 kcal·mol⁻¹· \AA^{-2} and 200 kcal·mol⁻¹·rad⁻², respectively. The value of the quartic van der Waals repulsion term [cf. eq 5 in Nilges et al. (1988a)] is calculated with a force constant of 4 kcal·mol⁻¹· \AA^{-4} with the hard-sphere van der Waals radii set to 0.8 times their standard values used in the CHARMM empirical energy function (Brooks et al., 1983). ^e E_{L-J} is the Lennard-Jones 6-12 van der Waals energy calculated with the CHARMM empirical energy function (Brooks et al., 1983). It is not included in the target function for simulated annealing and minimization. ^fThe improper torsion terms serve to maintain planarity and chirality; they also maintain the peptide bond of all residues in the trans conformation. ^gThe side-chain heavy atoms from the C γ position onward are excluded for Ser-13, Asn-24, Asp-26, Ser-28, Glu-45, and Lys-46 and from the C β position onward for Arg-17, Arg-18, Glu-22, Arg-41, Glu-42, and Asp-43.

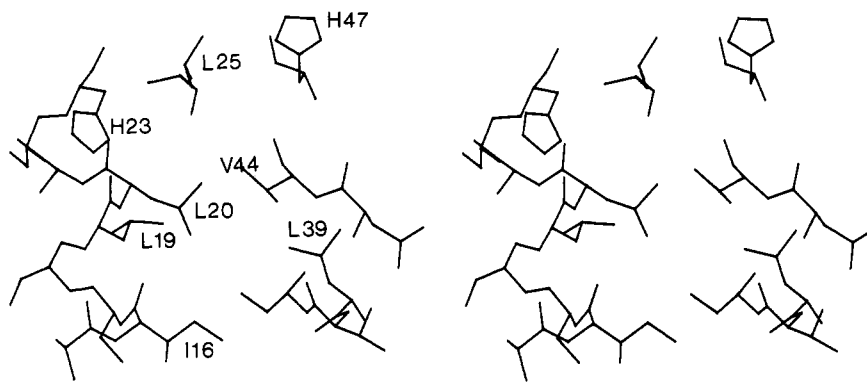


FIGURE 6: Stereoview of side chains in the hydrophobic core of the E3-binding domain of E2o.

shown. Proline commonly occurs at the N-termini of helices, so that Pro-14 may serve as an N-terminal boundary to further extension of helix I. In addition, it seems that the region from Leu-12 to Pro-14 represents the N-terminal boundary of the well-ordered E3-binding domain, as suggested both by the current structural data and by the high frequency of certain amino acids (Ala, Pro, Glx) characteristic of the interdomain flexible regions (Perham & Packman, 1989) in the other E2 sequences at the positions corresponding to the 11 disordered residues at the N-terminus. The only other position in which there is a preponderance of Pro in the aligned sequences is at position 35, which corresponds to the tip of the irregular loop. Interestingly, the mean ϕ angle found in the calculated structures for Val-35 is -62.9° and is relatively well-defined, with a mean angular deviation of only 16° ; thus, the ϕ angle

of Val-35 is compatible with the restricted ϕ angle found for prolines (Richardson, 1981), suggesting that a Pro at position 35 may adopt a similar conformation in this irregular loop.

Many of the most conservatively substituted residues are residues with basic or acidic side chains (Figure 7), most of which have substantial surface accessibility in the structure (Figure 4). Four positions are predominantly occupied by positively charged residues and two by negatively charged residues; these are the positions corresponding to Arg-17, Arg-18, Arg-38, Arg-41, Glu-22, and Asp-43. Of the charged residues, Arg-17, Arg-38, and Asp-43 are the most strictly conserved, with only the unusual protein component X sequence having a nonconservative Arg17 \rightarrow Ala17 substitution. Although Asp-43 is absolutely conserved, it is the only charged residue in the structure which has a relatively low solvent

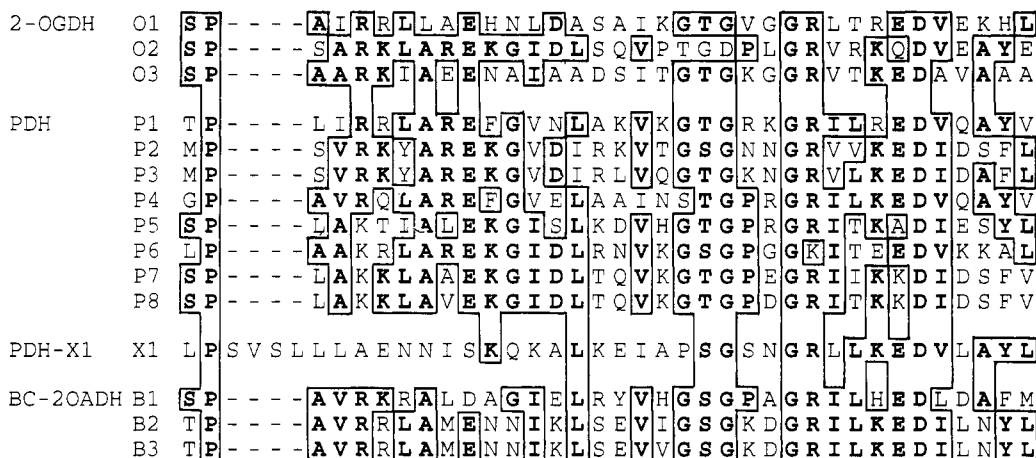


FIGURE 7: Aligned E3-binding domain sequences of E2o, E2p, E2b, and protein component X from several prokaryotic and eukaryotic species. O1, *E. coli* E2o (Spencer et al., 1984); O2, *Bacillus subtilis* E2o (Carlsson & Hederstedt, 1989); O3, *A. vinelandii* E2o (Westphal & de Kok, 1990); P1, *E. coli* E2p (Stephens et al., 1983); P2, *B. subtilis* E2p (Hemila et al., 1990); P3, *Bacillus stearothermophilus* E2p (Packman et al., 1988); P4, *A. vinelandii* E2p (Hanemaaijer et al., 1987); P5, *S. cerevisiae* E2p (Niu et al., 1988); P6, *Neurospora crassa* MRP3 (believed to be an E2 unit, possibly of PDH, from *N. crassa* mitochondrion) (Russel & Guest, 1991); P7, rat E2p (Gershwin et al., 1987); P8, human liver E2p (Thekkumkara et al., 1988); X1, *S. cerevisiae* protein component X (Behal et al., 1989); B1, *Ps. putida* E2b (Burns et al., 1988); B2 and B3, bovine and human E2b (Lau et al., 1988).

accessibility ($19.6 \pm 7.2\%$) in the calculated structure and clearly plays a role in stabilizing the structure through potential hydrogen bonds between its side-chain carboxylate and the backbone amides of Thr-33 and Thr-40, as well as the side-chain hydroxyl group of Thr-40 (Figure 5).

The remaining positions of the E3-binding domain are not conserved in the 15 sequences shown. Since these residues, however, have generally high surface accessibilities (Figure 4), they probably do not play a critical role in determining the polypeptide fold or the structure of the E2-E3 interface of the 2-oxo acid dehydrogenase complexes.

The high identity and sequence similarity in the aligned sequences is generally in agreement with other reports of alignment of the entire E2 chain. The initial report of the *Pseudomonas putida* E2b sequence, however, indicated no significant similarity between the E3-binding domain of *Ps. putida* E2b and *E. coli* E2o or E2p (Burns et al., 1988). On the basis of the present structure determination, we suggest that the correct alignment should be *E. coli* E2o (115-149), *E. coli* E2p (330-364), and *Ps. putida* (139-174), as proposed recently by Russel and Guest (1991). The current alignment shown in Figure 7 provides a cautionary example of the potential instabilities of sequence alignment algorithms, particularly when not based on three-dimensional experimental structures.

Implications for the Nature of the E3-E2 Interface. A few general criteria for assessing which residues are likely to be important participants in the E2-E3 interface can be advanced. First, the residues of the E3-binding domain which interact with E3 should have highly solvent-accessible side chains and are likely to occur in areas of high similarity in the aligned sequences. Second, as in general only one E3 chain for all 2-oxo acid dehydrogenases is produced within a single organism, it is likely that the contact residues are conserved in pairs of E2 chains from the same species. Third, it seems reasonable to suggest that electrostatic interactions (salt bridges and/or hydrogen bonds) are likely to be particularly prominent features of the E2-E3 interface. Fourth, the contact residues should form an approximately contiguous surface on the protein. On this basis, we suggest that the front surface of the two helices, in the view depicted in Figure 5, may be involved in the contact site through the conserved charged side chains: namely, Arg-17, Arg-18, and Glu-22 in helix I, Arg-38

at the end of the irregular loop leading into helix II, and Arg-41 and Glu-42 in helix II. Direct experimental analysis of the areas of contact between E3 and the E3-binding domain can now be undertaken to test this and other possibilities.

Registry No. E2o, 9032-28-4; E3, 9001-18-7; E1o, 9031-02-1; 51-residue synthetic peptide, 139375-81-8.

REFERENCES

- Bax, A. (1989) *Methods Enzymol.* 176, 151-158.
 Bax, A., Sklenar, V., Clore, G. M., & Gronenborn, A. M. (1987) *J. Am. Chem. Soc.* 109, 7188-7190.
 Behal, R. H., Browning, K. S., Hall, T. B., & Reed, L. J. (1989) *Proc. Natl. Acad. Sci. U.S.A.* 86, 8732-8736.
 Braunschweiler, L. R., & Ernst, R. R. (1983) *J. Magn. Reson.* 53, 521-528.
 Brooks, B. R., Brucoleri, R. E., Olafson, B. D., States, D. J., Swaminathan, S., & Karplus, M. (1983) *J. Comput. Chem.* 4, 187-217.
 Brown, S. C., Weber, P. L., & Mueller, L. (1987) *J. Magn. Reson.* 77, 166-169.
 Brünger, A. T. (1988) *XPLOR Manual*, Yale University, New Haven, CT.
 Brünger, A. T., Clore, G. M., Gronenborn, A. M., & Karplus, M. (1986) *Proc. Natl. Acad. Sci. U.S.A.* 83, 3801-3805.
 Burns, G., Brown, T., Hatter, K., & Sokatch, J. R. (1988) *Eur. J. Biochem.* 176, 165-169.
 Carlsson, P., & Hederstedt, L. (1989) *J. Bacteriol.* 171, 3667-3672.
 Clore, G. M., & Gronenborn, A. M. (1987) *Protein Eng.* 1, 275-288.
 Clore, G. M., & Gronenborn, A. M. (1989) *CRC Crit. Rev. Biochem. Mol. Biol.* 24, 479-564.
 Clore, G. M., & Gronenborn, A. M. (1991a) *Annu. Rev. Biophys. Biophys. Chem.* 20, 29-63.
 Clore, G. M., & Gronenborn, A. M. (1991b) *Science* 252, 1390-1399.
 Clore, G. M., Nilges, M., Sukuraman, D. K., Brünger, A. T., Karplus, M., & Gronenborn, A. M. (1986) *EMBO J.* 5, 2729-2735.
 Clore, G. M., Gronenborn, A. M., Nilges, M., & Ryan, C. A. (1987) *Biochemistry* 26, 8012-8023.
 Clore, G. M., Appella, E., Yamada, M., Matsushima, K., & Gronenborn, A. M. (1990) *Biochemistry* 29, 1689-1696.

- Clore, G. M., Wingfield, P. T., & Gronenborn, A. M. (1991) *Biochemistry* 30, 2315-2323.
- Dardel, F., Packman, L. C., & Perham, R. N. (1990) *FEBS Lett.* 264, 206-210.
- Dardel, F., Laue, E. D., & Perham, R. N. (1992) *Eur. J. Biochem.* (in press).
- Davis, D. G., & Bax, A. (1985) *J. Am. Chem. Soc.* 107, 2821-2822.
- DeRosier, D. J., & Oliver, R. M. (1971) *Cold Spring Harbor Symp. Quant. Biol.* 36, 199-203.
- DeRosier, D. J., Oliver, R. M., & Reed, L. J. (1971) *Proc. Natl. Acad. Sci. U.S.A.* 68, 1135-1137.
- Forman-Kay, J. D., Gronenborn, A. M., Kay, L. E., Wingfield, P. T., & Clore, G. M. (1990) *Biochemistry* 29, 1566-1572.
- Forman-Kay, J. D., Clore, G. M., Wingfield, P. T., & Gronenborn, A. M. (1991) *Biochemistry* 30, 2685-2698.
- Gershwin, M. E., McKay, I. R., Sturgess, A., & Coppel, R. L. (1987) *J. Immunol.* 138, 3525-3531.
- Gronenborn, A. M., Filpula, D. R., Essig, N. Z., Achari, A., Whitlow, M., Wingfield, P. T., & Clore, G. M. (1991) *Science* 253, 657-661.
- Hanemaaijer, R., de Kok, A., Jolles, J., & Veeger, C. (1987) *Eur. J. Biochem.* 169, 245-252.
- Havel, T. F. (1986) DISGEO, Quantum Chemistry Program Exchange No. 507, Indiana University, Bloomington, IN.
- Havel, T. F., & Wüthrich, K. (1984) *Bull. Math. Biol.* 46, 673-698.
- Hemila, H., Palva, A., Paulin, L., Arvidson, S., & Palva, I. (1990) *J. Bacteriol.* 172, 5052-5063.
- Jeener, J., Meier, B. H., Bachmann, P., & Ernst, R. R. (1979) *J. Chem. Phys.* 71, 4546-4553.
- Kraulis, P. J. (1991) *J Appl. Crystallogr.* 24, 946-950.
- Kraulis, P. J., Clore, G. M., Nilges, M., Jones, T. A., Petterson, G., Knowles, J., & Gronenborn, A. M. (1989) *Biochemistry* 28, 7241-7257.
- Lau, K. S., Griffin, T. A., Hu, C. W. C., & Chuang, D. T. (1988) *Biochemistry* 27, 1972-1981.
- Marion, D., & Wüthrich, K. (1983) *Biochem. Biophys. Res. Commun.* 113, 967-974.
- Marion, D., & Bax, A. (1988) *J. Magn. Reson.* 80, 528-533.
- Mattevi, A., Schierbeeck, A. J., & Hol, W. G. J. (1991) *J. Mol. Biol.* 220, 975-994.
- Merrifield, R. B., Vizili, L. D., & Boman, H. G. (1982) *Biochemistry* 21, 5020-5031.
- Mueller, L. (1987) *J. Magn. Reson.* 72, 191-196.
- Nilges, M., Clore, G. M., & Gronenborn, A. M. (1988a) *FEBS Lett.* 229, 317-324.
- Nilges, M., Gronenborn, A. M., Brünger, A. T., & Clore, G. M. (1988b) *Protein Eng.* 2, 27-38.
- Nilges, M., Clore, G. M., & Gronenborn, A. M. (1988c) *FEBS Lett.* 239, 129-136.
- Nilges, M., Clore, G. M., & Gronenborn, A. M. (1990) *Biopolymers* 29, 813-822.
- Niu, X., Browning, K. S., Behal, R. H., & Reed, L. J. (1988) *Proc. Natl. Acad. Sci. U.S.A.* 85, 7546-7550.
- Oliver, R. M., & Reed, L. J. (1982) in *Electron Microscopy of Proteins* (Harris, J. R., Ed.) Vol. 2, pp 1-48, Academic Press, London.
- Omichinski, J. G., Clore, G. M., Appella, E., Sakaguchi, K., & Gronenborn, A. M. (1990) *Biochemistry* 29, 9324-9334.
- Packman, L. C., & Perham, R. N. (1986) *FEBS Lett.* 206, 193-198.
- Packman, L. C., & Perham, R. N. (1987) *Biochem. J.* 242, 531-538.
- Packman, L. C., Borges, A., & Perham, R. N. (1988) *Biochem. J.* 252, 79-86.
- Patel, M. S., & Roche, T. E. (1990) *FASEB J.* 4, 3224-3233.
- Perham, R. N. (1991) *Biochemistry* 30, 8501-8512.
- Perham, R. N., & Packman, L. C. (1989) *Ann. N.Y. Acad. Sci.* 573, 1-20.
- Plateau, P., & Gueron, M. (1982) *J. Am. Chem. Soc.* 104, 7310-7311.
- Radford, S. E., Laue, E. D., Perham, R. N., Martin, S. R., & Appella, E. (1989a) *J. Biol. Chem.* 264, 767-775.
- Radford, S. E., Perham, R. N., Ullrich, S. J., & Appella, E. (1989b) *FEBS Lett.* 250, 336-340.
- Reed, L. J. (1974) *Acc. Chem. Res.* 7, 40-46.
- Reed, L. J., & Hackert, M. L. (1990) *J. Biol. Chem.* 265, 8971-8974.
- Richardson, J. S. (1981) *Adv. Protein Chem.* 34, 167-339.
- Russell, G. C., & Guest, J. R. (1991) *Biochim. Biophys. Acta* 1076, 225-232.
- Spencer, M. E., Darlinson, M. G., Stephens, P. E., Duckenfield, I. K., & Guest, J. R. (1984) *Eur. J. Biochem.* 141, 361-374.
- Stephens, P. E., Darlinson, M. G., Lewis, H. M., & Guest, J. R. (1983) *Eur. J. Biochem.* 133, 481-489.
- Takenaka, A., Kizawa, K., Hata, T., Sato, S., Misaka, E.-J., Tamura, C., & Sasada, Y. (1988) *J. Biochem. (Tokyo)* 103, 463-469.
- Tam, J. P., Heath, W. F., & Merrifield, R. B. (1983) *J. Am. Chem. Soc.* 105, 6442-6445.
- Texter, F. L., Radford, S. E., Laue, E. D., Perham, R. N., Miles, J. S., & Guest, J. R. (1988) *Biochemistry* 27, 289-296.
- Thekkumkara, T. J., Ho, L., Wexler, I. R., Pons, G., Liu, T. C., & Patel, M. S. (1988) *FEBS Lett.* 240, 45-48.
- Wagenknecht, T., Francis, N., DeRosier, D. J., Hainfeld, J. F., & Wall, J. S. (1987) *J. Biol. Chem.* 262, 877-882.
- Wagenknecht, T., Grassucci, R., & Schaak, D. (1990) *J. Biol. Chem.* 265, 22402-22408.
- Wagner, G., Braun, W., Havel, T. F., Schaumann, T., Go, N., & Wüthrich, K. (1987) *J. Mol. Biol.* 196, 611-639.
- Westphal, A. H., & de Kok, A. (1990) *Eur. J. Biochem.* 187, 235-239.
- Williamson, M. P., Havel, T. F., & Wüthrich, K. (1985) *J. Mol. Biol.* 182, 295-315.
- Wüthrich, K. (1986) *NMR of Proteins and Nucleic Acids*, John Wiley, New York.
- Wüthrich, K., Billeter, M., & Braun, W. (1983) *J. Mol. Biol.* 169, 949-961.
- Yang, H., Hainfeld, J. F., Wall, J. S., & Frey, P. A. (1985) *J. Biol. Chem.* 260, 16049-16051.
- Zar, J. H. (1984) *Biostatistical Analysis*, Prentice-Hall, Englewood Cliffs, CA.